Anti-obesity and immunostimulatory activity of *Chrysosplenium flagelliferum* in mouse preadipocytes 3T3-L1 cells and mouse macrophage RAW264.7 cells

JEONG WON CHOI[1*], GWANG HUN PARK[2*], HYEOK JIN CHOI[1], JAE WON LEE[1], HAE-YUN KWON[2], MIN YEONG CHOI[2] and JIN BOO JEONG[1]

[1]Department of Forest Science, Andong National University, Andong, Gyeongsangbuk 36729, Republic of Korea; [2]Forest Medicinal Resources Research Center, National Institute of Forest Science, Yeongju, Gyeongsangbuk 36040, Republic of Korea

Received April 4, 2024; Accepted May 22, 2024

DOI: 10.3892/etm.2024.12604

Abstract. *Chrysosplenium flagelliferum* (CF) is known for its anti-inflammatory, antioxidant and antibacterial activities. However, there is a lack of research on its other pharmacological properties. In the present study, the bifunctional roles of CF in 3T3-L1 and RAW264.7 cells were investigated, focusing on its anti-obesity and immunostimulatory effects. In 3T3-L1 cells, CF effectively mitigated the accumulation of lipid droplets and triacylglycerol. Additionally, CF downregulated the peroxisome proliferator-activated receptor (PPAR)-γ and CCAAT/enhancer-binding protein α protein levels; however, this effect was impeded by the knockdown of β-catenin using β-catenin-specific small interfering RNA. Consequently, CF-mediated inhibition of lipid accumulation was also decreased. CF increased the protein levels of adipose triglyceride lipase and phosphorylated hormone-sensitive lipase, while decreasing those of perilipin-1. Moreover, CF elevated the protein levels of phosphorylated AMP-activated protein kinase and PPARγ coactivator 1-α. In RAW264.7 cells, CF enhanced the production of pro-inflammatory mediators, such as nitric oxide (NO), inducible NO synthase, interleukin (IL)-1β, IL-6 and tumor necrosis factor-α, and increased their phagocytic capacities. Inhibition of Toll-like receptor (TLR)-4 significantly reduced the effects of CF on the production of pro-inflammatory mediators and phagocytosis, indicating its crucial role in facilitating these effects. CF-induced increase in the production of pro-inflammatory mediators was controlled by the activation of c-Jun N-terminal kinase (JNK) and nuclear factor (NF)-κB pathways, and TLR4 inhibition attenuated the phosphorylation of these kinases. The results of the pesent study suggested that CF inhibits lipid accumulation by suppressing adipogenesis and inducing lipolysis and thermogenesis in 3T3-L1 cells, while stimulating macrophage activation via the activation of JNK and NF-κB signaling pathways mediated by TLR4 in RAW264.7 cells. Therefore, CF simultaneously exerts both anti-obesity and immunostimulatory effects.

Correspondence to: Professor Jin Boo Jeong, Department of Forest Science, Andong National University, 1375 Gyeongdong-ro, Andong, Gyeongsangbuk 36729, Republic of Korea
E-mail: jjb0403@anu.ac.kr

[*]Contributed equally

Key words: *Chrysosplenium flagelliferum*, anti-obesity, immunostimulatory activity, adipocytes, macrophages

Introduction

Obesity is characterized by the excessive accumulation of body fat due to the imbalance between energy intake and expenditure (1). Excessive accumulation of body fat, leading to obesity, is attributed to an increase in both the size and number of adipocytes differentiated from preadipocytes (2). Obesity, a precursor to various metabolic disorders such as type 2 diabetes, cardiovascular diseases, non-alcoholic fatty liver disease and cancer, is a global health concern owing its role in the etiology of various conditions (3). Furthermore, obesity leads to infectious diseases by weakening the immune system, thereby increasing the risk of infection by foreign pathogens and/or worsening the patient prognosis, ultimately increasing the mortality rate (4,5). Obese patients exhibited high infection and mortality rates during the coronavirus disease-2019 (COVID-19) pandemic (6). Therefore, obesity treatment is important for protection from such viral pandemics. To date, numerous pharmaceuticals, such as orlistat, lorcaserin, phentermine/topiramate and liraglutide, have been developed for obesity treatment. However, these medications induce various side effects, such as flatus with discharge, insomnia, dysgeusia, nausea and headache, affecting their long-term use (7). Consequently, natural product-based supplements without side effects have been extensively studied for obesity treatment. Owing to increasing health consciousness, natural substances are preferred for the development of anti-obesity products (8).

Chrysosplenium flagelliferum (CF), belonging to family *Saxifragaceae*, is a plant mainly found in the Northern Hemisphere regions, such as Russia, China, Japan and South Korea (9). CF is traditionally used to treat inflammation (10).

Methanol extract of CF has been revealed to exert antioxidant and antibacterial effects against *Propionibacterium acnes* (10). However, the pharmacological efficacy of CF and its potential therapeutic effects remain largely unexplored. CF is listed as an approved food ingredient by the Ministry of Food and Drug Safety of the Republic of Korea, and no adverse effects associated with its use have been reported to date. Therefore, the aim of the present study was to assess the pharmacological efficacy of CF by evaluating its anti-obesity and immunostimulatory effects and explore the underlying mechanisms using a cell-based approach *in vitro* to facilitate the development of new functional agents.

Materials and methods

Chemical reagents. Dexamethasone, 3-isobutyl-1-methylxanthine (IBMX), insulin, Oil red O, PD98059 [extracellular signal-regulated kinase (ERK)-1/2 inhibitor], SB203580 (p38 inhibitor), SP600125 [c-Jun N-terminal kinase (JNK) inhibitor], C29 [Toll-like receptor (TLR)2 inhibitor], TAK-242 (TLR4 inhibitor) referred to as TAK hereafter and BAY 11-7082 [BAY; nuclear factor (NF)-κB inhibitor] were purchased from MilliporeSigma. Primary antibodies against the peroxisome proliferator-activated receptor (PPAR)-γ (cat. no. 2435), CCAAT/enhancer-binding protein α (CEBPα; cat. no. 8178), adipose triglyceride lipase (ATGL; cat. no. 2138), hormone-sensitive lipase (HSL; cat. no. 4107), phosphorylated (p)-HSL (cat. no. 4137), perilipin-1 (cat. no. 9349), AMP-activated protein kinase, catalytic, α-1 (AMPKα also known as AMPK; cat. no. 5831), p-AMPKα (cat. no. 2535), and β-actin (cat. no. 5125), as well as horseradish peroxidase-conjugated anti-rabbit (cat. no. 7074) and anti-mouse IgG (cat. no. 7076) secondary antibodies were purchased from Cell Signaling Technology, Inc. The primary antibody against PPARγ coactivator 1-α (PGC-1α; cat. no. sc-518025) was purchased from Santa Cruz Biotechnology, Inc. Control small interfering RNA (siRNA; cat. no. 6568) and β-catenin siRNA (cat. no. sc-29210) were purchased from Cell Signaling Technology Inc. and Santa Cruz Biotechnology, Inc., respectively.

Sample preparation. CF was obtained as a dehydrated powder from the National Institute of Forest Science (Seoul, South Korea). To prepare the extract, distilled water, with a volume 20-fold that of CF, was added to 10 g of CF. This mixture underwent a 24-h extraction process in a water bath at 60˚C. The resultant extract was lyophilized, re-dissolved in distilled water, and subsequently used in cellular assays.

Cell culture. RAW264.7 murine macrophages (cat. no. TIB-71) and 3T3-L1 mouse preadipocytes (cat. no. CL-173) were obtained from the American Type Culture Collection. Culture of RAW264.7 cells was conducted in a controlled CO_2 incubator environment (37˚C, 5% CO_2) using Dulbecco's modified Eagle's medium/nutrient mixture F-12 (DMEM/F-12) (cat. no. SH3023.01; Cytiva), supplemented with 10% fetal bovine serum (FBS) (cat. no. 16000-044; Gibco; Thermo Fisher Scientific, Inc.) and a combination of penicillin (100 U/ml) and streptomycin (100 μg/ml). Additionally, 3T3-L1 cells were propagated under similar conditions (37˚C, 5% CO_2) in DMEM/F-12 medium supplemented with 10% bovine calf serum (cat. no. 16170-078; Gibco; Thermo Fisher Scientific, Inc.) and penicillin/streptomycin combination.

Measurement of the viability of RAW264.7 and 3T3-L1 cells. Cell viability was assessed via 3-(4,5-dimethylthiazol-2-yl)-2,5-diphenyltetrazolium bromide (MTT) assay. RAW264.7 and 3T3-L1 cells (at >90% confluence in the wells), following CF treatment (50-200 μg/ml), were incubated for 24 h and 8 days, respectively, in 96-well plates at 37˚C. Following incubation, the cells were treated with the MTT reagent (1 mg/ml) and incubated for 4 h at 37˚C. After the addition of dimethyl sulfoxide, the cells were incubated for 10 min at room temperature. Finally, absorbance of the resulting solution was measured at 570 nm using the UV/visible spectrophotometer (Xma-3000PC; Human Corporation).

Differentiation of 3T3-L1 cells. A total of 2 days after reaching full confluence [designated as day 0 (D0)] in a 6-well culture plate, 3T3-L1 preadipocytes were induced to differentiate. Briefly, the cells (at 100% confluence in the wells) were incubated in DMEM/F-12 enriched with DMI cocktail (0.05 mM IBMX, 1 μM dexamethasone, and 10 μg/ml insulin) until D2 at 37˚C. The cells were then cultured for 2 more days in DMEM/F-12 supplemented with 10 μg/ml insulin until D4 at 37˚C. The culture continued from D6 to D8 at 37˚C, and the medium was renewed every other day.

Transfection with siRNA. The 3T3-L1 cells ($2x10^6$ cells/well) were plated in a 6-well plate and incubated overnight to achieve adherence. Subsequently, the cells were transfected with the control-siRNA (Cell Signaling Technology Inc.) and β-catenin-siRNA (Santa Cruz Biotechnology, Inc.), each at a concentration of 100 nM. Transfection was performed for 48 h using the TransIT-TKO transfection reagent (Mirus Bio), according to the manufacturer's protocol. Control-siRNA was used as non-targeting siRNA for the negative control. Immediately following the completion of siRNA transfection, cell differentiation was initiated.

Oil red O staining of 3T3-L1 cells. Under differentiation, cells were treated with CF for D0-D8, D0-D2, or D8-D10 and the concentration of CF used in the experiments ranged from 50 to 200 μg/ml in the dose-dependent studies, while it was set at 200 μg/ml in all other cases. Following treatment, 3T3-L1 cells were fixed with 10% formalin at an ambient temperature for 1 h. Following fixation, the cells were rinsed thrice with distilled water and dehydrated using 60% isopropanol for 5 min at room temperature. Fully dehydrated 3T3-L1 cells were subjected to Oil red O staining for 20 min at room temperature for lipid droplet visualization. After staining, the cells were rinsed twice with distilled water and examined under a light microscope (Olympus Corporation) at a magnification of x400. To quantify the accumulated lipid droplets, Oil red O was extracted from the stained lipid droplets in completely dried cells using 100% isopropanol. Finally, absorbance was measured at 500 nm using the microplate reader (Xma-3000PC).

Measurement of glycerol levels in 3T3-L1 cells. Upon reaching maximum confluency in a 6-well plate, 3T3-L1 cells

(at 100% confluence in the wells) were cultured for an additional 2 days. Post this period (D0), the cells were mixed with DMI (0.05 mM IBMX, 1 μM dexamethasone and 10 μg/ml insulin) and incubated for 2 days (D2). The 3T3-L1 cells were then exposed to insulin (10 μg/ml) and cultured for another 2 days (D4). The cells were further cultured for 4 days, with the medium refreshed every other day (D6-D8). Following differentiation, the 3T3-L1 cells were treated with CF (200 μg/ml) and were incubated for 2 days (D8-D10). All the steps were performed at a constant temperature of 37˚C in a 5% CO_2 environment. After 2 days of CF treatment (D10), free glycerol content was evaluated using a Glycerol Cell-Based Assay Kit (cat. no. 10011725; Cayman Chemical Company), according to the manufacturer's instructions. Briefly, the cell culture medium was mixed with the prepared free glycerol assay reagent at a 1:4 ratio and incubated at room temperature for 15 min. Subsequently, absorbance was measured at 540 nm using the microplate reader (Xma-3000PC).

Measurement of nitric oxide (NO) levels in RAW264.7 cells. RAW264.7 cells (1x10^5 cells/well) were propagated in a 96-well culture plate in DMEM/F-12 supplemented with 10% FBS. The cells were exposed to CF for 24 h at 37˚C. In addition, the cells were pretreated with C29 (100 μM, TLR2 inhibitor), TAK (5 μM, TLR4 inhibitor), PD (20 μM, ERK1/2 inhibior), SB (20 μM, p38 inhibitor), SP (20 μM, JNK inhibitor) or BAY (10 μM, NF-κB inhibitor) at 37˚C for 2 h and then co-treated with CF (200 μg/ml) at 37˚C for 24 h. To quantify NO levels, the culture medium was mixed with the Griess reagent (cat. no. G4410-10G; MilliporeSigma) and incubated for 15 min at ambient temperature. Absorbance of the resulting mixture was measured at 540 nm using the UV/visible spectrophotometer (Xma-3000PC). The concentration of CF used in the experiments ranged from 50 to 200 μg/ml in the dose-dependent studies, while it was set at 200 μg/ml in all other cases.

Measurement of phagocytotic activity in RAW264.7 cells. Phagocytic activity in RAW264.7 cells was assessed using the neutral red uptake method. The cells (at over 90% confluence in the wells) were cultured in DMEM/F-12 enriched with 10% FBS and treated with CF (50-200 μg/ml) at 37˚C for 24 h. In addition, the cells were pretreated with C29 (100 μM, TLR2 inhibitor) or TAK (5 μM, TLR4 inhibitor) at 37˚C for 2 h and then co-treated with CF (200 μg/ml) at 37˚C for 24 h. For phagocytic assessment, the cells were stained with 0.01% neutral red at 37˚C for 2 h and treated with a lysis solution (50:50 mixture of ethanol and 1% acetic acid) to extract neutral red at room temperature. Absorbance of the released dye was measured at 540 nm using the UV/visible spectrophotometer (Xma-3000PC) to assess the extent of phagocytic uptake.

Reverse transcription-polymerase chain reaction (RT-PCR) analysis. RAW264.7 cells (at >90% confluence in the wells) were treated with CF for 24 h in the presence or absence of chemical inhibitors. The concentration of CF used in the experiments ranged from 50 to 200 μg/ml in the dose-dependent studies, while it was set at 200 μg/ml in all other cases. Total RNA was carefully extracted from RAW264.7 cells using the RNeasy Mini Kit (Qiagen, Inc.). RNA (1 μg) was subsequently reverse-transcribed into cDNA using the Verso cDNA Kit (Thermo Fisher Scientific Inc.). RT-PCR analysis was performed targeting inducible NO synthase (iNOS), interleukin (IL)-1β, IL-6, tumor necrosis factor (TNF)-α, and glyceraldehyde-3-phosphate dehydrogenase (GAPDH) using the prepared cDNA and PCR Master Mix Kit (Promega Corporation). All primers used for amplification are listed in Table I. PCR cycles (30 in total) were executed in a PCR Thermal Cycler Dice (Takara Bio, Inc.) as follows: Denaturation at 94˚C for 30 sec, annealing at 55˚C for 1 min, and extension at 72˚C for 1 min. The amplified products were electrophoresed on a 1% agarose gel at 100 V for 15 min. The DNA bands on the agarose gel were visualized using Safe Shine Green (10,000X) (cat. no. G6051; Biosesang). Band intensities were quantitatively analyzed using the UN-SCAN-IT 5.1 software (Silk Scientific, Inc). GAPDH was used as a loading control for normalization in RT-PCR analysis.

Table I. Sequences of primers used in the amplification of cDNA.

Primers	Sequences
iNOS	Forward, 5'-TTGTGCATCGACCTAGGCTG GAA-3'
	Reverse, 5'-GACCTTTCGCATTAGCATGGA AGC-3'
IL-1β	Forward, 5'-GGCAGGCAGTATCACTCATT-3'
	Reverse, 5'-CCCAAGGCCACAGGTATTT-3'
IL-6	Forward, 5'-GAGGATACCACTCCCAACAG ACC-3'
	Reverse, 5'-AAGTGCATCATCGTTGTTCAT ACA-3'
TNF-α	Forward, 5'-TGGAACTGGCAGAAGAGGCA-3'
	Reverse, 5'-TGCTCCTCCACTTGGTGGTT-3'
GAPDH	Forward, 5'-GGACTGTGGTCATGAGCCCTT CCA-3'
	Reverse, 5'-ACTCACGGCAAATTCAACGG CAC-3'

iNOS, inducible NO synthase; IL, interleukin; TNF-α, tumor necrosis factor-α; GAPDH, glyceraldehyde-3-phosphate dehydrogenase.

Western blot analysis. Under differentiation, 3T3-L1 cells were treated with CF for D0-D8, D0-D2, D0-D4 or D8-D10. The concentration of CF used in the experiments ranged from 100 to 200 μg/ml in the dose-dependent studies, while it was set at 200 μg/ml in all other cases. RAW264.7 cells were treated with CF (200 μg/ml) for 1-6 h in the absence of TAK (5 μM) or were treated with CF (200 μg/ml) for 3 h in the presence of TAK (5 μM) at 37˚C. After washing with phosphate-buffered saline, proteins were extracted from RAW264.7 and 3T3-L1 cells using a radioimmunoprecipitation assay buffer (cat. no. BP-115DG; Boston BioProducts, Inc.). The resulting lysates were centrifuged at 4˚C and 25,200 x g for 30 min. Protein concentrations were quantified using the bicinchoninic acid assay kit (Thermo Fisher

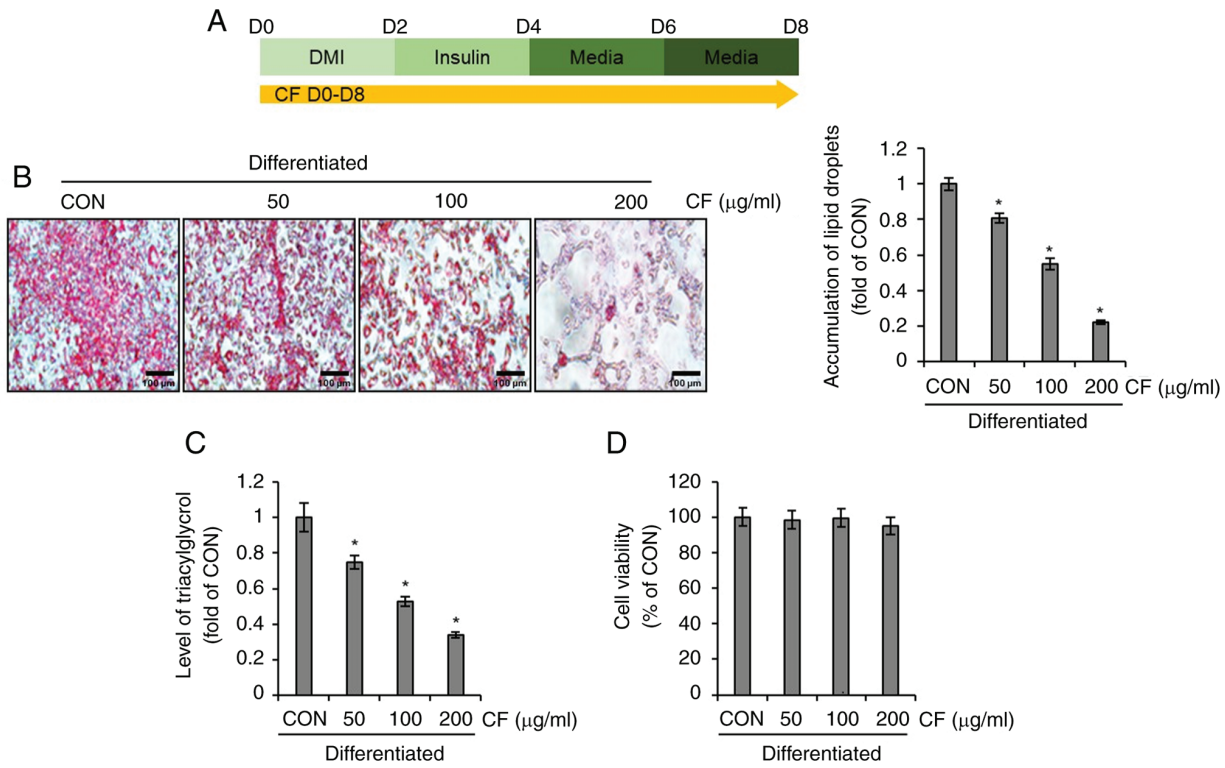

Figure 1. Effect of CF on the accumulation of lipid droplets and triacylglycerol in 3T3-L1 cells. CF was administered to 3T3-L1 cells undergoing differentiation induced by DMI and insulin, from D0 to D8. Subsequently, the extent of lipid accumulation, the content of triacylglycerol and cell viability were measured. (A) Experimental design. (B) Oil Red O staining (magnification, x400), (C) triacylglycerol content and (D) cell viability in CF-treated 3T3-L1 cells. *P<0.05 vs. CON. CF, *Chrysosplenium flagelliferum*; DMI, dexamethasone, 3-isobutyl-1-methylxanthine, insulin; D, day; CON, control.

Scientific, Inc.). For electrophoresis, 30 μg of protein from each sample was loaded per well, resolved via 10% sodium dodecyl sulfate-polyacrylamide gel electrophoresis and transferred to a nitrocellulose membrane (Thermo Fisher Scientific, Inc.). Membranes were blocked with 5% skimmed milk for 1 h at room temperature and incubated overnight with primary antibodies in a 5% bovine serum albumin (BSA) solution (1:1,000 dilution) at 4°C. Subsequently, the membranes were incubated with 5% BSA solution with secondary antibodies (1:1,000 dilution) for 1 h at room temperature. An ECL Select™ Western Blotting Detection Reagent (cat. no. RPN2232; Cytiva) was then added to visualize the horseradish peroxidase activity. Protein bands were visualized using the LI-COR C-DiGit Blot Scanner (LI-COR Biosciences) and quantitatively analyzed using UN-SCAN-IT gel software version 5.1 (Silk Scientific, Inc.). Actin was used as a loading control for normalization in western blot analysis.

Statistical analysis. All experiments were repeated at least three times. Statistical analyses were conducted using GraphPad Prism v.5.0 (GraphPad; Dotmatics), and data are presented as the mean ± standard deviation. All data were analyzed using one-way analysis of variance, followed by Bonferroni's post-hoc test. P<0.05 was considered to indicate a statistically significant difference.

Results

Effect of CF on lipid droplet accumulation in 3T3-L1 cells. To investigate whether CF inhibits lipid droplet accumulation in differentiated 3T3-L1 cells, the differentiation of 3T3-L1 cells was induced using DMI and insulin while administering CF from D0 to D8. Subsequently, the extent of lipid formation and triglyceride accumulation was analyzed (Fig. 1A). As illustrated in Fig. 1B and C, CF significantly reduced the accumulation of lipid droplets and triglycerides in differentiated 3T3-L1 cells. To ascertain whether the inhibition of lipid droplets and triglyceride accumulation mediated by CF is due to its cytotoxic effects on 3T3-L1 cells, the impact of CF on cellular viability was evaluated. CF exerted no detrimental effect on 3T3-L1 cell survival (Fig. 1D).

Effect of CF on the adipogenic differentiation of 3T3-L1 cells. To evaluate whether CF inhibits adipogenic differentiation in 3T3-L1 cells, differentiation was induced by the use of DMI and insulin while administering CF from D0 to D8. Subsequently, western blot analysis was conducted to determine the expression levels of adipogenic differentiation-related molecules, PPARγ and CEBPα. At 100 μg/ml, CF did not decrease the protein levels of PPARγ and CEBPα. However, at 200 μg/ml, CF significantly reduced the protein levels of PPARγ and CEBPα (Fig. 2A). Considering the necessity of PPARγ and CEBPα for the differentiation of preadipocytes into adipocytes, which is marked by the accumulation of lipid droplets (11,12), it was investigated whether CF reduces the protein levels of PPARγ and CEBPα during this critical differentiation stage. First, the differentiation of preadipocytes into adipocytes was induced using DMI while administering CF from D0 to D2. Subsequently, western blot analysis was conducted to assess the alterations in the protein levels of

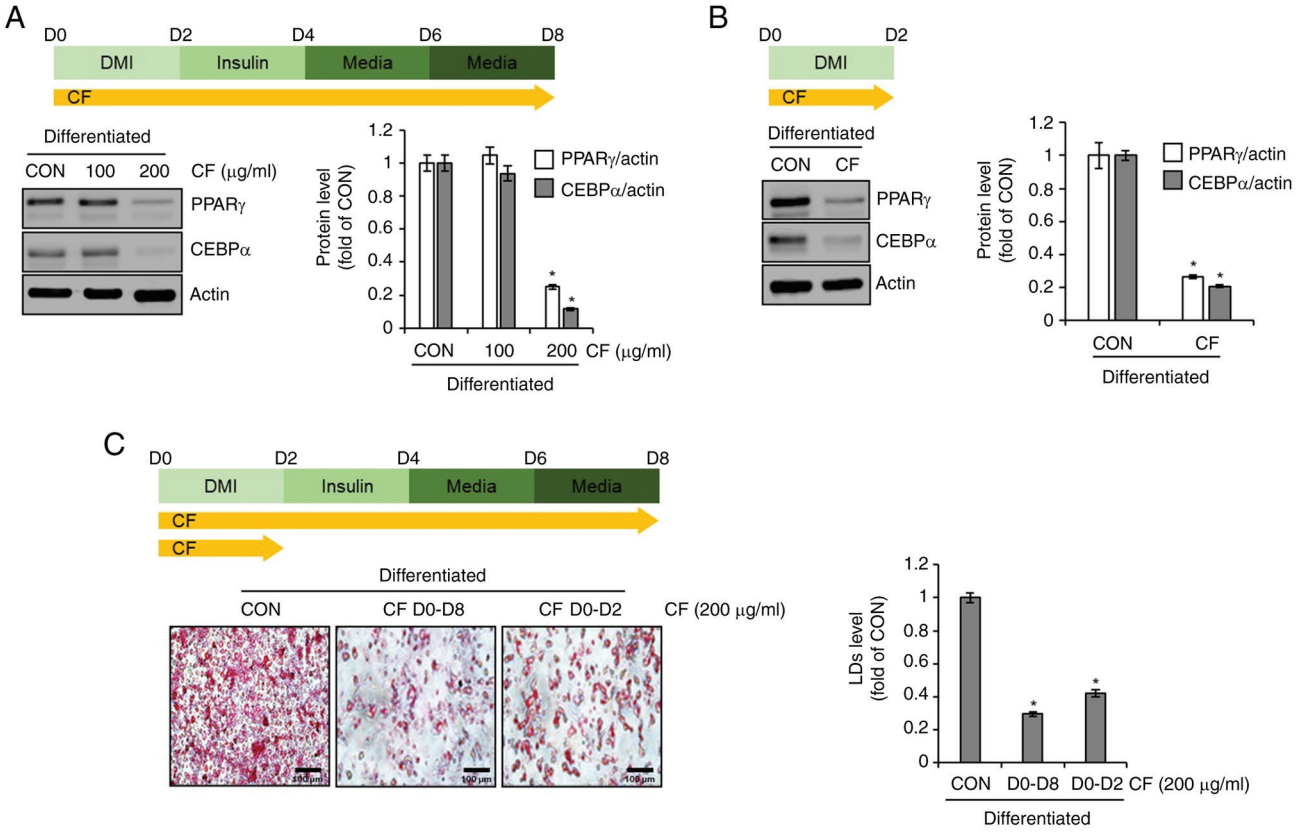

Figure 2. Effect of CF on the expression of adipogenic markers in 3T3-L1 cells. (A) CF was administered to 3T3-L1 cells undergoing differentiation induced by DMI and insulin, from D0 to D8. Experimental design and western blot analysis of PPARγ and CEBPα in 3T3-L1 cells treated with CF (D0-D8). (B) CF (200 μg/ml) was administered to 3T3-L1 cells undergoing differentiation induced by DMI, from D0 to D2. Experimental design and western blot analysis of PPARγ and CEBPα in 3T3-L1 cells treated with CF (D0-D2). (C) CF was administered to 3T3-L1 cells undergoing differentiation induced by DMI and insulin, from D0 to D8 or from D0 to D2. Experimental design and Oil Red O staining (magnification, x400) in 3T3-L1 cells treated with CF (D0-D8 or D0-D2). *P<0.05 vs. CON. CF, *Chrysosplenium flagelliferum*; D, day; DMI, dexamethasone, 3-isobutyl-1-methylxanthine, insulin; PPARγ, peroxisome proliferator-activated receptor gamma; CEBPα, CCAAT/enhancer-binding protein α; CON, control; LDs, lipid droplets.

PPARγ and CEBPα induced by CF. CF significantly reduced the protein levels of PPARγ and CEBPα during the differentiation from preadipocytes to adipocytes (Fig. 2B). To determine whether the inhibition of preadipocyte differentiation to adipocytes by CF results in decreased lipid droplet accumulation, the extent of lipid accumulation was compared after treatment with CF from D0 to D8 and D0 to D2. As revealed in Fig. 2C, a notable reduction in lipid accumulation was observed in the 3T3-L1 cells treated with CF from D0 to D2 or from D0 to D8. Furthermore, the reduction of the accumulation in the D0 to D8 group was greater than that in the D0 to D2 group.

Effect of β-catenin on CF-mediated inhibition of adipogenic differentiation in 3T3-L1 cells. To investigate the impact of CF on the protein levels of β-catenin in 3T3-L1 cells, CF was administered from D0 to D2 and from D0 to D4. Subsequently, western blot analysis was used to assess the alterations in the protein levels of β-catenin induced by CF. As illustrated in Fig. 3A, CF increased the protein levels of β-catenin in a time-dependent manner. To further ascertain the impact of increased β-catenin protein levels induced by CF on the protein levels of PPARγ and CEBPα, the changes in PPARγ and CEBPα protein levels were analyzed in 3T3-L1 cells after β-catenin knockdown using the β-catenin siRNA. Western blot analysis revealed that CF significantly reduced the protein levels of PPARγ and CEBPα in 3T3-L1 cells without β-catenin knockdown (Fig. 3B). However, in 3T3-L1 cells with β-catenin knockdown, CF significantly decreased the protein levels of PPARγ and CEBPα, but to a more modest degree than the cells without β-catenin knockdown (Fig. 3B). To further evaluate whether the inhibition of the CF-mediated decrease in the protein levels of PPARγ and CEBPα due to β-catenin knockdown affects the CF-mediated suppression of lipid droplet accumulation, β-catenin-knockdown 3T3-L1 cells were treated with CF from D0 to D2 and lipid droplet accumulation was analyzed on D8. As revealed in Fig. 3C, treatment of cells without β-catenin knockdown with CF resulted in a notable decrease in lipid droplet accumulation. However, in cells with β-catenin knockdown, the CF-mediated inhibitory effect on lipid droplet accumulation was significantly diminished.

Effects of CF on lipolysis and thermogenesis in 3T3-L1 cells. To explore the effects of CF on lipolysis and thermogenesis in 3T3-L1 cells, the cells were treated with CF from D0 to D8 during the differentiation process. Subsequently, western blotting was conducted to assess the changes in protein levels of lipolysis-related molecules, such as ATGL, p-HSL, HSL, perilipin-1 and thermogenesis-related molecules, such as p-AMPK, AMPK and PGC-1α. As illustrated in Fig. 4A, 3T3-L1 cells treated with CF exhibited a concentration-dependent increase

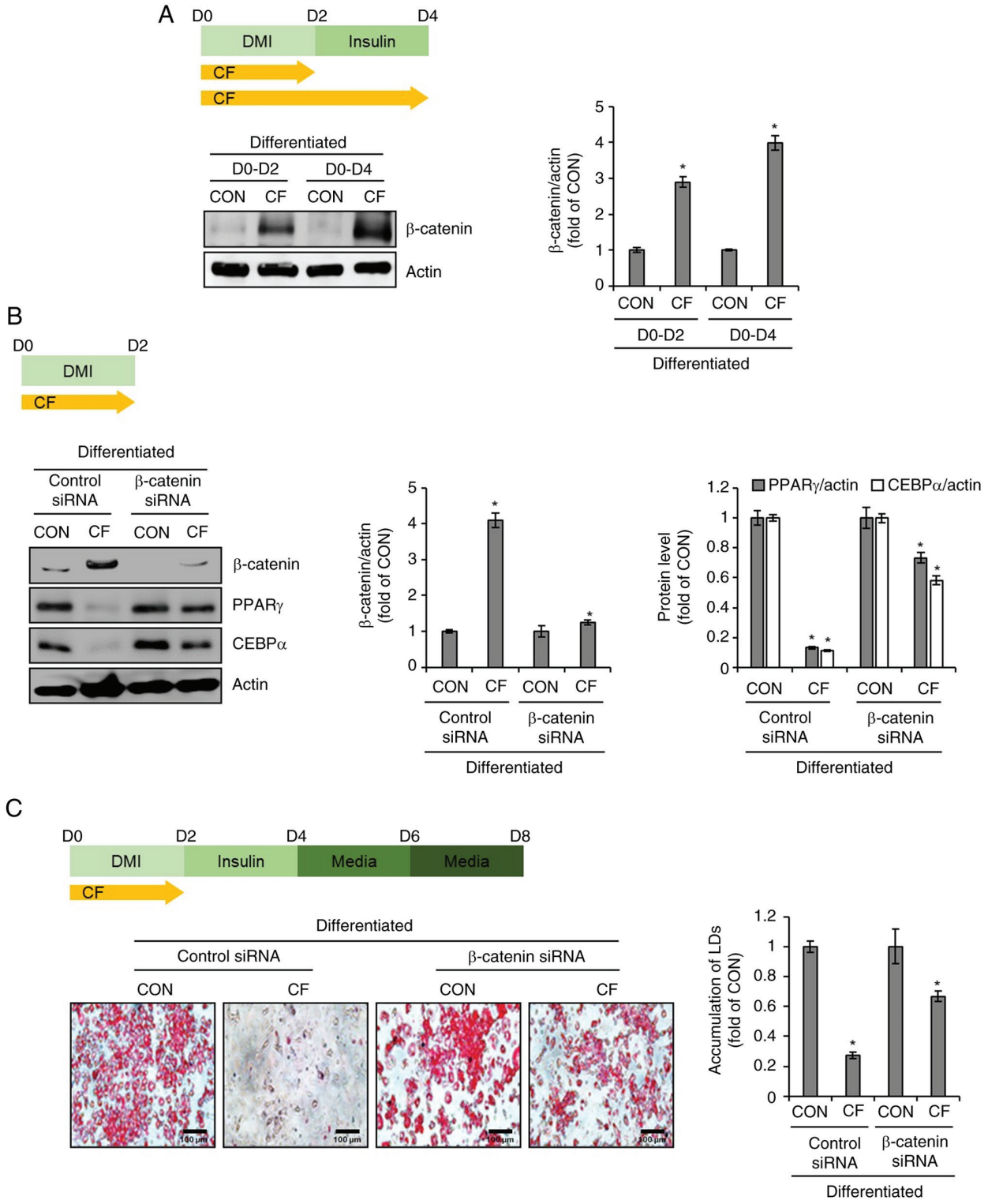

Figure 3. Effect of CF on β-catenin expression in 3T3-L1 cells. (A) CF (200 μg/ml) was administered to 3T3-L1 cells undergoing differentiation induced by DMI and insulin, from D0 to D2 or D0 to D4. Experimental design and western blot analysis of β-catenin in 3T3-L1 cells treated with CF (D0-D2 or D0-D4). (B) CF (200 μg/ml) was administered to β-catenin-knock downed 3T3-L1 cells undergoing differentiation induced by DMI and insulin, from D0 to D2. Experimental design and western blot analysis of PPARγ and CEBPα in β-catenin-knockdown 3T3-L1 cells treated with CF (D0-D2). (C) CF (200 μg/ml) was administered to β-catenin-knockdown 3T3-L1 cells undergoing differentiation induced by DMI and insulin, from D0 to D2. Experimental design and Oil Red O staining (magnification, x400) in β-catenin-knockdown 3T3-L1 cells treated with CF (D0-D2). *P<0.05 vs. CON. CF, *Chrysosplenium flagelliferum*; D, day; DMI, dexamethasone, 3-isobutyl-1-methylxanthine, insulin; CON, control; siRNA, small interfering RNA; PPARγ, peroxisome proliferator-activated receptor gamma; CEBPα, CCAAT/enhancer-binding protein α; LDs, lipid droplets.

in ATGL and the ratio of p-HSL to HSL, whereas perilipin-1 levels decreased. Additionally, CF treatment led to an increase in the ratio of p-AMPK to AMPK and PGC-1α. Thus, to determine whether the induction of lipolysis and thermogenesis mediated by CF contributes to the reduction in accumulated lipid droplets, the cells were treated with CF from D8 to D10,

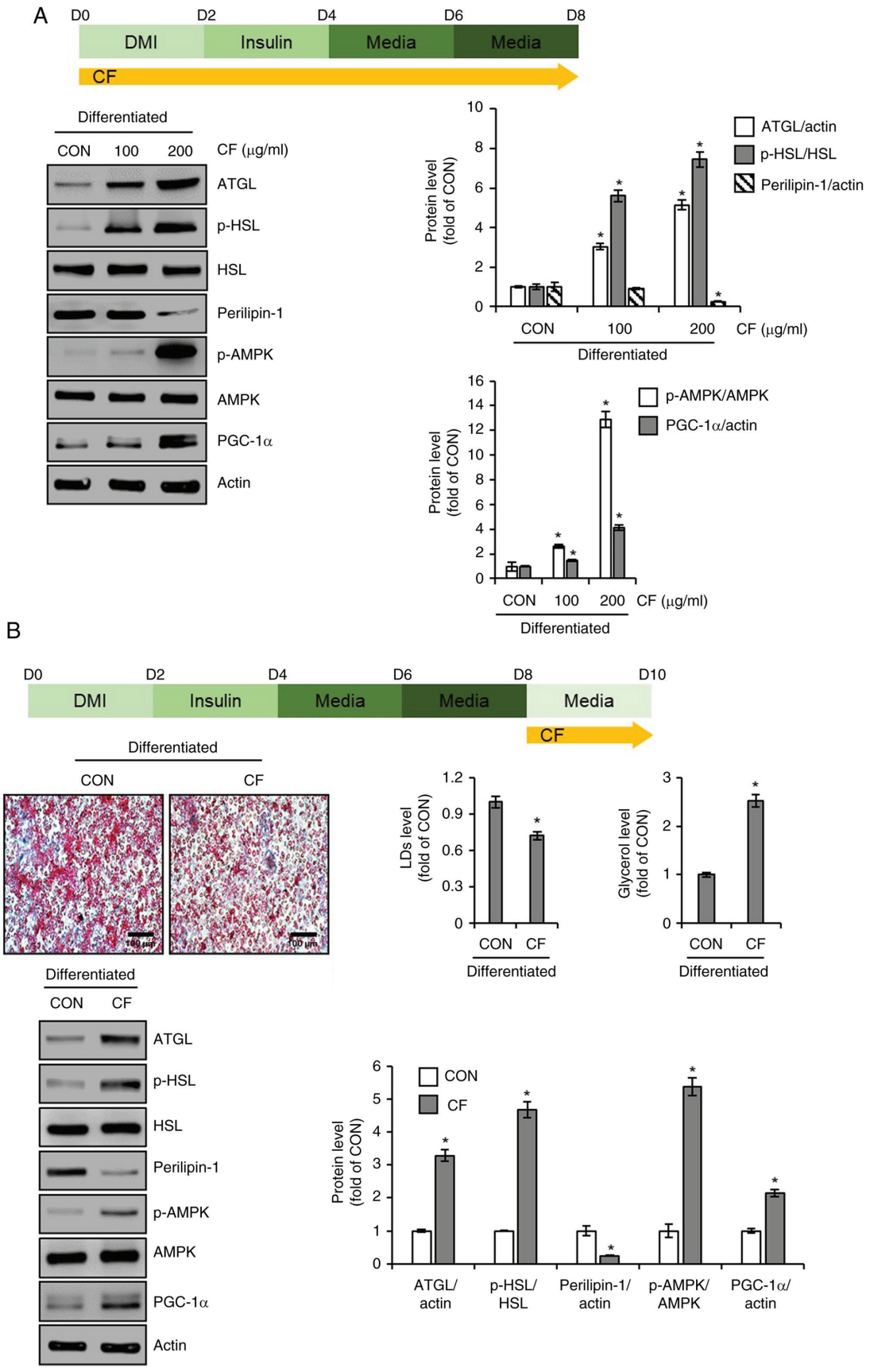

Figure 4. Effect of CF on the expression of lipolytic and thermogenic markers in 3T3-L1 cells. (A) CF (200 μg/ml) was administered to 3T3-L1 cells undergoing differentiation induced by DMI and insulin, from D0 to D8. Experimental design and western blot analysis of ATGL, p-HSL, HSL, perilipin-1, p-AMPK, AMPK, and PGC-1α in 3T3-L1 cells treated with CF (D0-D8). (B) CF (200 μg/ml) was administered to differentiated 3T3-L1 by DMI and insulin, from D8 to D10. Experimental design, Oil Red O staining (magnification, x400), glycerol level, and western blot analysis of ATGL, p-HSL, perilipin-1, p-AMPK, and PGC-1α in 3T3-L1 cells treated with CF (D8-D10). *P<0.05 vs. CON. CF, *Chrysosplenium flagelliferum*; DMI, dexamethasone, 3-isobutyl-1-methylxanthine, insulin; D, day; ATGL, adipose triglyceride lipase; p-, phosphorylated; HSL, hormone-sensitive lipase; AMPK, AMP-activated protein kinase; PGC-1α, peroxisome proliferator-activated receptor-γ coactivator 1α; CON, control.

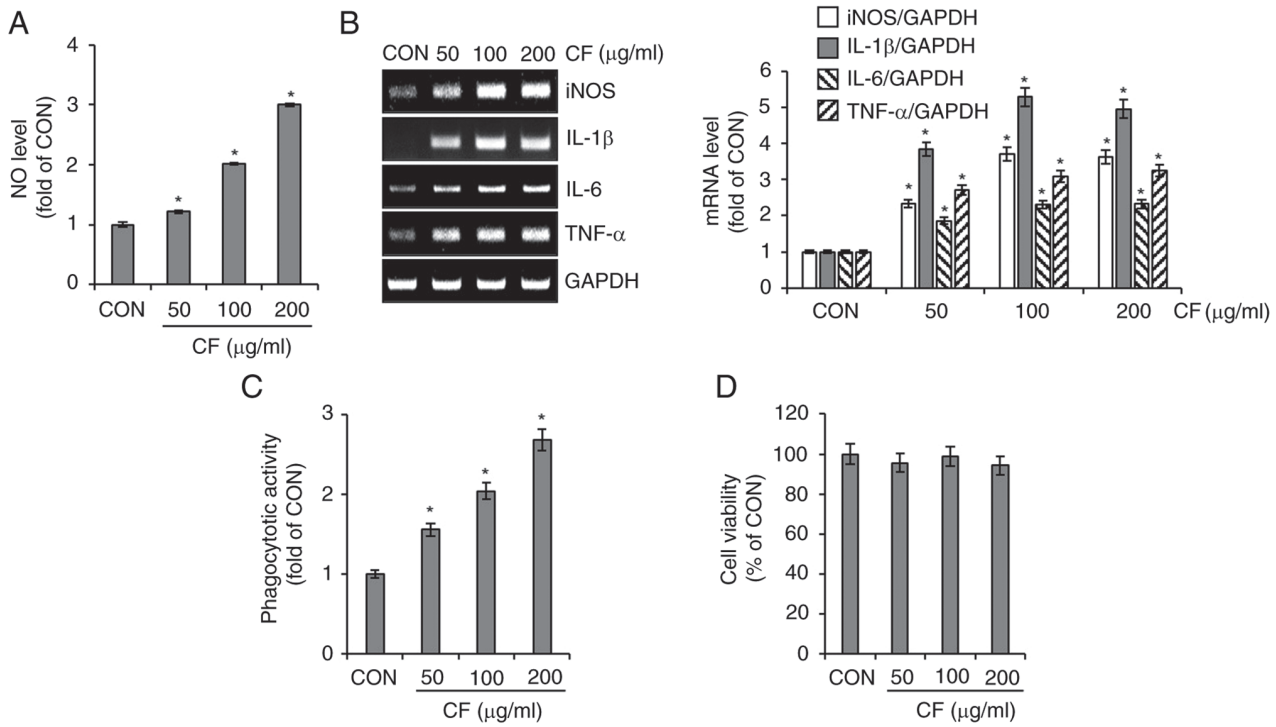

Figure 5. Effect of CF on macrophage activation in RAW264.7 cells. (A) CF was administered to RAW264.7 cells for 24 h. The level of NO was measured using Griess assay. (B) CF was administered to RAW264.7 cells for 24 h. The mRNA levels of iNOS, IL-1β, IL-6 and TNF-α were measured using reverse transcription PCR. (C) CF was administered to RAW264.7 cells for 24 h. Phagocytotic activity was measured using the neutral red uptake method. (D) CF was administered to RAW264.7 cells for 24 h. Cell viability was measued using MTT assay. *P<0.05 vs. CON. CF, *Chrysosplenium flagelliferum*; NO, nitric oxide; iNOS, inducible nitric oxide synthase; IL-1β, interleukin-1β; IL-6, interleukin-6; TNF-α, tumor necrosis factor-α; CON, control.

whereas lipid accumulation was induced without CF treatment from D0 to D8. Subsequently, the changes in lipid accumulation, glycerol release and protein levels of molecules related to lipolysis and thermogenesis were analyzed. As depicted in Fig. 4B, treatment of cells with complete lipid accumulation with CF resulted in a decrease in accumulated lipids and an increase in glycerol levels. Furthermore, CF treatment led to an increase in the levels of lipolysis-related molecules, such as ATGL and p-HSL, and a decrease in perilipin-1 (Fig. 4B). Additionally, CF enhanced the levels of thermogenesis-related molecules, including p-AMPK and PGC-1α (Fig. 4B).

Effect of CF on macrophage activation in RAW264.7 cells. To investigate the immunostimulatory activity of CF, its effect on macrophage activation was analyzed in RAW264.7 cells. As shown in Fig. 5A and B, cells treated with CF exhibited a significant increase in the secretion of NO and the expression of iNOS, IL-1β, IL-6 and TNF-α. Furthermore, CF significantly enhanced the phagocytic activity of RAW264.7 cells (Fig. 5C). However, CF did not exhibit cytotoxic effects on RAW264.7 cells (Fig. 5D).

Effects of TLR2 and TLR4 on CF-mediated activation of RAW264.7 macrophages. To evaluate the impact of TLR2 and TLR4 on CF-mediated activation of macrophages, RAW264.7 cells were treated with CF, where TLR2 and TLR4 were inhibited using C29sp16 and TAK, respectively. Subsequently, the changes in the levels of NO, the expression of iNOS, IL-1β and TNF-α, as well as alterations in phagocytic activity were analyzed. As illustrated in Fig. 6A, compared with untreated cells (CON group), cells treated solely with CF (DM group) exhibited a notable increase in NO production, whereas the inhibition of TLR2 by C29 only slightly suppressed CF-mediated NO production. However, the inhibition of TLR4 by TAK resulted in an almost complete absence of CF-mediated NO production. The expression of iNOS, IL-1β and TNF-α mediated by CF was slightly decreased by the inhibition of TLR2 but significantly reduced by the inhibition of TLR4 (Fig. 6B). Furthermore, it was observed that the activation of phagocytic activity in RAW264.7 cells mediated by CF was more substantially reduced by the inhibition of TLR4 than by the inhibition of TLR2 (Fig. 6C).

Effects of mitogen-activated protein kinase (MAPK) and NF-κB signaling pathways on CF-mediated activation of RAW264.7 macrophages. To investigate the effects of MAPK and NF-κB signaling pathways on CF-mediated activation of macrophages, RAW264.7 cells were treated with CF and with the inhibitors of each signaling pathway. Subsequently, the changes in NO production and the expression of iNOS, IL-1β and TNF-α were examined. As demonstrated in Fig. 7A, the inhibition of ERK1/2 by PD had no effect on CF-mediated NO production. However, the inhibition of p38 by SB and the inhibition of JNK by SP both suppressed CF-mediated NO production, with the suppression due to JNK inhibition being particularly pronounced. Therefore, the impact of JNK inhibition by SP on the expression of iNOS, IL-1β and TNF-α mediated by CF was analyzed. The results revealed that the inhibition of JNK significantly decreased the CF-mediated expression of iNOS, IL-1β and TNF-α (Fig. 7B). Furthermore,

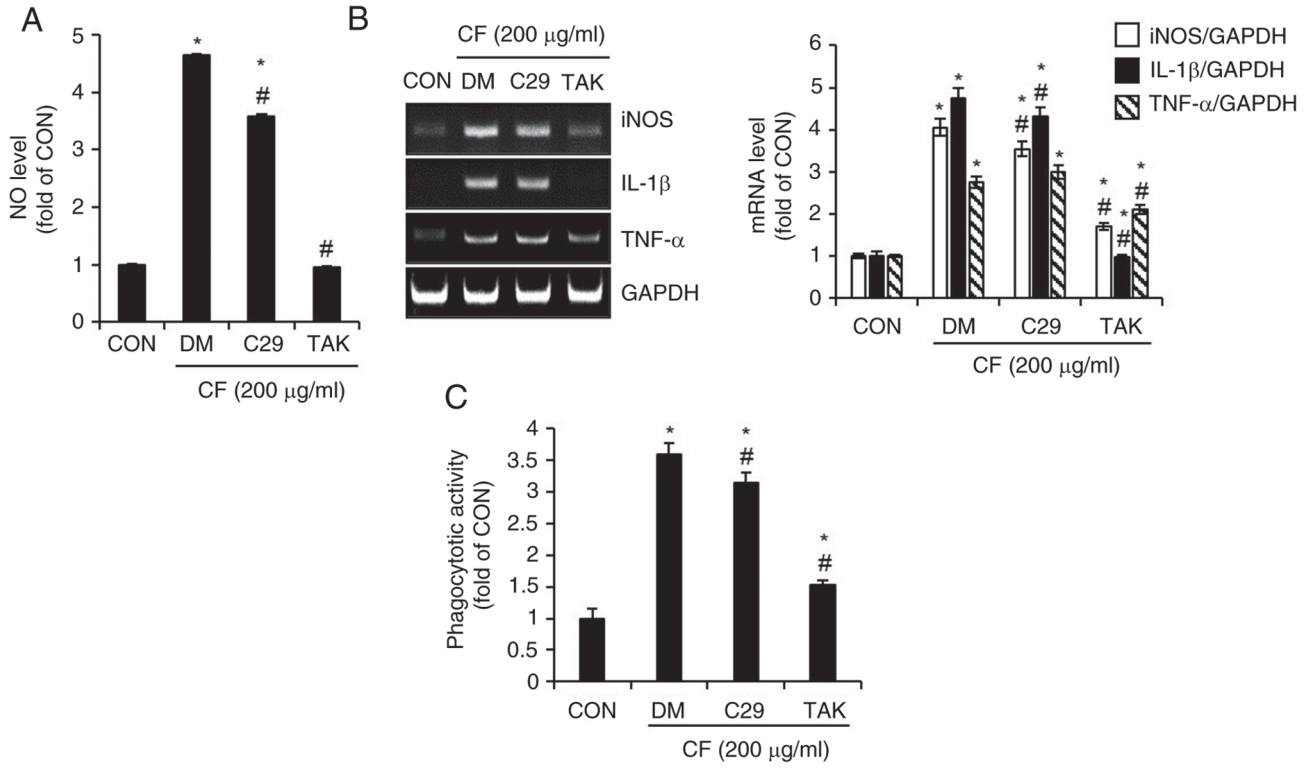

Figure 6. Effect of TLR2 and TLR4 on CF-mediated activation of macrophages in RAW264.7 cells. RAW264.7 cells were pretreated with C29 (TLR2 inhibitor, 100 μM) or TAK (TLR4 inhibitor, 5 μM) for 2 h and then co-treated with CF (200 μg/ml) for 24 h. (A) The level of NO, (B) reverse transcription PCR analysis of iNOS, IL-1β and TNF-α, and (C) phagocytotic activity in RAW264.7 cells treated with CF for 24 h in the presence of C29 or TAK. *P<0.05 vs. CON. $^{\#}$P<0.05 vs. DM. TLR, toll-like receptor; CF, *Chrysosplenium flagelliferum*; TAK, TAK-242; NO, nitric oxide; iNOS, inducible nitric oxide synthase; IL-1β, interleukin-1β; TNF-α, tumor necrosis factor-α; CON, control; DM, DMSO group.

it was confirmed that the inhibition of NF-κB by BAY also resulted in a significant decrease in the CF-mediated production of NO and the expression of iNOS, IL-1β and TNF-α (Fig. 7C). Thus, it was then investigated whether CF activated the JNK and NF-κB signaling pathways. The results indicated that CF increases the phosphorylation of JNK and p65, which are the active forms of JNK and NF-κB signaling, respectively (Fig. 7D). As the activation of macrophages mediated by CF primarily occurs via TLR4 stimulation, it was analyzed whether the activation of JNK and NF-κB by CF is influenced by TLR4. Inhibition of TLR4 by TAK significantly suppressed the CF-mediated phosphorylation of JNK and p65 (Fig. 7E).

Discussion

In the human body, excess energy is stored in adipocytes in the form of lipids via a process that is a hallmark of obesity (11). Obesity is characterized by the enlargement of existing adipocytes and increase in the number of new adipocytes due to preadipocyte differentiation (11). To investigate the potential anti-obesity effects of CF, the changes in lipid accumulation within adipocytes after CF treatment were examined in the present study. A significant reduction in lipid accumulation in the adipocytes treated with CF was observed. However, CF did not exert any adverse effects on adipocyte viability. These findings suggested the anti-obesity activity of CF and highlighted its potential as a safe and effective agent to combat obesity. Lack of a detrimental effect on adipocyte viability further underscored its suitability as a therapeutic agent for obesity management. Adipogenesis, differentiation of preadipocytes into mature adipocytes, plays a key role in increasing the number of lipid-storing adipocytes (11). Consequently, adipogenesis inhibition has been used as a molecular target for the discovery of new anti-obesity agents, underlining its significance in obesity research and treatment (11). In the present study, to evaluate the inhibitory effect of CF on adipogenesis, preadipocytes undergoing differentiation into adipocytes were treated with CF. Post-treatment, western blot analysis was employed to assess the expression changes of PPARγ and C/EBPα, key regulators instrumental in the activation of adipogenesis (12). PPARγ has been demonstrated to be essential for both adipogenesis and the maintenance of adipocyte phenotype, as evidenced through *in vivo* and *ex vivo* studies (13-16). Similarly, C/EBPα has been proven to be crucial for the differentiation and maintenance of white adipose tissue, also validated through *in vivo* and *ex vivo* experiments (17-20). These existing reports collectively indicate that the suppression of PPARγ and C/EBPα expression can effectively inhibit adipogenesis. In the present study, it was revealed that CF inhibits the expression of PPARγ and C/EBPα, which in turn leads to the suppression of lipid accumulation within adipocytes. These results demonstrate that the anti-obesity activity of CF may primarily operate through the suppression of adipogenesis, mediated by the inhibition of PPARγ and C/EBPα expression. Activation of the Wnt signaling pathway inhibits the expression of PPARγ and C/EBPα, thereby maintaining preadipocytes in an undifferentiated state and suppressing adipogenesis. Conversely, inhibition of Wnt signaling induces

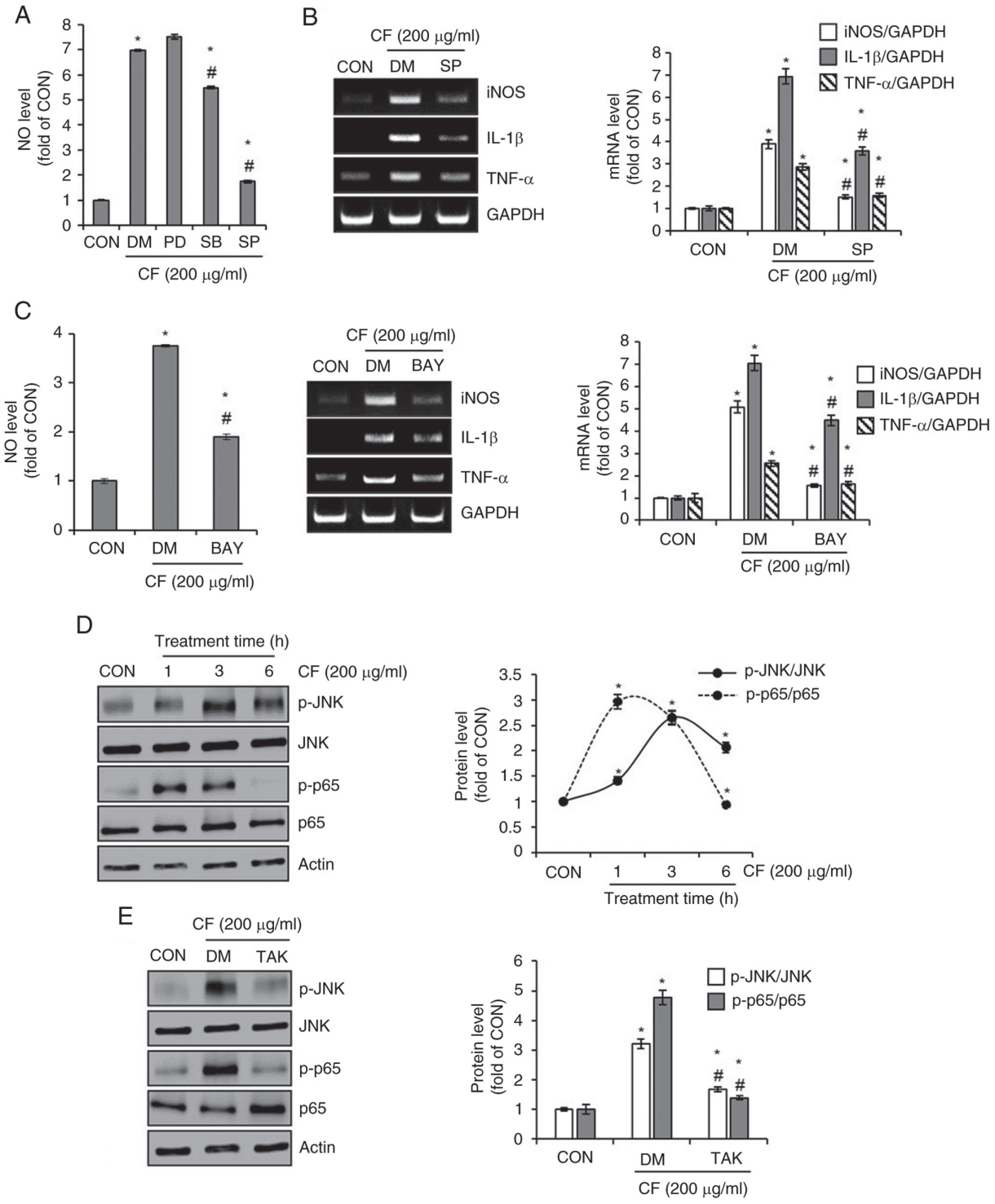

Figure 7. Effect of MAPK and NF-κB signaling pathways on CF-mediated activation of macrophages in RAW264.7 cells. (A) RAW264.7 cells were pretreated with PD (ERK1/2 inhibitor, 20 μM), SB (p38 inhibitor, 20 μM) or SP (JNK inhibitor, 20 μM) and then co-treated with CF (200 μg/ml) for 24 h. The level of NO and (B) RT-PCR analysis of iNOS, IL-1β and TNF-α in RAW264.7 cells treated with CF in the presence of PD, SB or SP. (C) RAW264.7 cells were pretreated with BAY (NF-κB inhibitor, 10 μM), and then co-treated with CF (200 μg/ml) for 24 h. The level of NO and RT-PCR analysis of iNOS, IL-1β, and TNF-α in RAW264.7 cells treated with CF for 24 h in the presence of BAY. (D) RAW264.7 cells were treated with CF (200 μM) for the indicated time-points. Western blot analysis of p-JNK, JNK, p-p65 and p65 in RAW264.7 cells treated with CF. (E) RAW264.7 cells were pretreated with TAK (TLR4 inhibitor, 5 μM) for 2 h and the co-treated with CF (200 μM) for 3 h. Western blot analysis of p-JNK, JNK, p-p65, and p65 in RAW264.7 cells treated with CF in the presence of TAK. *P<0.05 vs. CON. $^{\#}$P<0.05 vs. DM. CF, *Chrysosplenium flagelliferum*; PD, PD98059; SB, SB203580; SP, SP600125; NO, nitric oxide; iNOS, inducible nitric oxide synthase; IL-1β, interleukin-1β; TNF-α, tumor necrosis factor-α; BAY, BAY11-7082; p-, phosphorylated; JNK, c-Jun N-terminal kinase; TAK, TAK-242; CON, control; DM, DMSO group.

adipogenic differentiation (21). During adipogenic differentiation, the degradation of β-catenin leads to an increase in the expression of PPARγ and C/EBPα. However, an elevation in β-catenin levels, even under conditions favoring adipogenic differentiation, results in decreased expression of PPARγ and C/EBPα, thereby inhibiting adipogenesis (22). Therefore,

to determine whether the CF-induced decrease in PPARγ and C/EBPα is associated with Wnt signaling, adipocytes undergoing adipogenic differentiation were treated with CF. Subsequently, western blot analysis was conducted to assess the changes in the levels of β-catenin protein. The results revealed that CF treatment led to an increase in the levels of β-catenin protein. Furthermore, in adipocytes where β-catenin was knocked down by siRNA, the CF-mediated decrease in PPARγ and C/EBPα was notably attenuated. This observation also led to the discovery that such β-catenin knockdown by siRNA consequently reduced the CF-mediated inhibition of lipid accumulation. These results indicated that CF inhibits adipogenesis through the activation of Wnt signaling, leading to the suppression of PPARγ and C/EBPα expression. However, a limitation of this study is the inability to ascertain whether the CF-mediated increase in β-catenin protein levels is due to the inhibition of proteasomal degradation or a result of transcriptional activation. Consequently, further mechanistic studies are required to elucidate the specific pathway involved in the CF-mediated elevation of β-catenin protein levels. It has been reported that the most ideal mechanism for anti-obesity treatments encompasses the augmentation of lipolysis and the enhancement of energy expenditure (23). Lipolysis is a catabolic reaction in which triacylglycerol stored in adipocytes is hydrolyzed to glycerol and fatty acids (24). During lipolysis, triacylglycerol is progressively hydrolyzed to diacylglycerol, monoacylglycerol, and glycerol by a series of lipolytic enzymes (25). ATGL catalyzes the hydrolysis of triacylglycerol to diacylglycerol, which is subsequently hydrolyzed to monoacylglycerol by HSL (26). As ATGL and HSL account for >90% of the triacylglycerol hydrolysis (26), they are considered pivotal indicators of lipolysis (27-29). Furthermore, perilipin-1, which encircles lipid droplets within adipocytes, has been revealed to play a role in lipolysis (30,31). Perilipin-1 was shown to inhibit lipolysis while concurrently promoting lipid synthesis and lipid droplet formation (32). Furthermore, perilipin-1 was demonstrated to lead to increased lipolysis, resulting in a reduction in the size of lipid droplets within adipocytes (33). In the present study, CF increased the protein levels of ATGL and p-HSL in adipocytes, while concurrently reducing the protein levels of perilipin-1. Upon treatment of lipid-laden adipocytes with CF, a reduction in the number of lipid droplets and an increase in glycerol content were observed. These findings indicated that CF can induce lipolysis, suggesting that its lipolytic action may contribute to the inhibition of lipid accumulation. Lipolysis in white adipose tissue is essential for thermogenesis (34). Furthermore, it has been reported that the browning of white adipose tissue can facilitate thermogenesis, thereby promoting energy expenditure (35). AMPK, a critical metabolic sensor and regulator of energy balance, induces browning of white adipose tissue (36). PGC-1α, known as a master transcriptional coactivator in mitochondrial biogenesis, is widely used as a key indicator for the differentiation of white adipose tissue into brown adipocytes (37). In the present study, it was confirmed that CF increases the protein levels of p-AMPK and PGC-1α in adipocytes. Although the current study did not analyze the impact of CF on the protein levels of uncoupling protein-1 and PR domain containing 16, closely associated with the browning of white adipocytes, which presents a limitation, the observed increase in the protein levels of p-AMPK and PGC-1α by CF can be considered evidence suggesting that CF may induce the browning of white adipocytes.

Macrophages maintain homeostasis by defending against foreign pathogens, processing internal waste and facilitating tissue repair (38). When foreign pathogens invade the human body, activated macrophages, as a key component of the innate immune system, phagocytize these invaders and secrete pro-inflammatory mediators, such as NO, iNOS, IL-1β, IL-6 and TNF-α (38). Furthermore, macrophages possess the ability to present antigens to adaptive immune cells, such as T and B cells, and pro-inflammatory mediators secreted by macrophages contribute to the activation of these T and B cells (39). In conclusion, these studies may serve as evidence suggesting that the activation of macrophages can play a positive role in both innate and adaptive immune responses. In the present study, it was confirmed that CF enhances the production of pro-inflammatory mediators, such as NO, iNOS, IL-1β, IL-6 and TNF-α, in macrophages and activates their phagocytic activity. These findings provided evidence that CF induces macrophage activation. Although this study did not elucidate the relationship between CF-mediated activation of macrophages and adaptive immune cells, such as T and B cells, which is a limitation, existing research that macrophage activation can induce T and B cell activation (39) suggests that CF may contribute to the activation of these cells through its role in macrophage activation. The inflammatory response of macrophages to eliminate foreign pathogens initiates upon the recognition of these pathogens by macrophages (38). Macrophages recognize pathogen-associated molecular patterns of foreign pathogens via pattern recognition receptors (PRRs) (38). Among the various PRRs in macrophages, TLRs play a pivotal role in the recognition of foreign pathogens (38). TLR2 and TLR4 play crucial roles in the elimination of foreign pathogens by inducing the production of proinflammatory mediators and activating phagocytic activity in macrophages (40). In the present study, it was observed that inhibition of TLR4 in cells resulted in a significant decrease in CF-mediated pro-inflammatory mediator production and phagocytic activation compared with cells with inhibition of TLR2. Although the present study did not fully analyze the relationship between CF-mediated macrophage activation and all PRRs present in macrophages, which is a limitation, the findings suggested that TLR4 plays a central role in the activation of macrophages mediated by CF. TLR4-mediated macrophage activation involves the signaling pathways of NF-κB and MAPK (41). In the current study, it was observed that the inhibition of JNK, a component of the MAPK signaling pathway, and NF-κB notably reduced the production of CF-mediated pro-inflammatory mediators, and the inhibition of TLR4 suppressed CF-mediated activation of JNK and NF-κB. These findings may serve as evidence that CF-mediated macrophage activation can be attributed to the activation of the TLR4-dependent JNK and NF-κB signaling pathways.

In the present study, it was found that CF inhibited adipogenesis and induced lipolysis and thermogenesis, thereby suppressing excessive lipid accumulation in adipocytes. Additionally, CF stimulated macrophage activation via TLR4-dependent activation of the JNK and NF-κB signaling

pathways. These findings indicated that CF exerts anti-obesity and immunostimulatory effects. Combined with the previously reported antioxidant and antimicrobial effects, the anti-obesity and immunostimulatory effects demonstrated in the present study expand the known pharmacological activity spectrum of CF. However, this study primarily relied on *in vitro* cellular assays and lacked *in vivo* experiments using animal models, representing a major limitation. Therefore, future *in vivo* studies using animal models are necessary to verify these findings and facilitate the development of new functional materials for the anti-obesity and immunostimulatory applications of CF.

Acknowledgements

Not applicable.

Funding

The present study was funded by the National Institute of Forest Science, Korea (grant no. FP0802-2023-01-2 023), the R&D Program for Forest Science Technology (grant no. RS-2024-00405196) provided by the Korea Forest Service (Korea Forestry Promotion Institute, Seoul, Korea).

Availability of data and materials

The data generated in the present study may be requested from the corresponding author.

Authors' contributions

JWC, GHP, HJC, JWL, HYK and MYC performed cell-based experiments and analyzed the data. JWC and GHP wrote the manuscript. JBJ designed the experiments and wrote and edited the manuscript. JWC, GHP, HJC, JWL, HYK, MYC and JBJ confirm the authenticity of all the raw data. All the authors have read and approved the final version of the manuscript.

Ethics approval and consent to participate

Not applicable.

Patient consent for publication

Not applicable.

Competing interests

The authors declare that they have no competing interests.

References

1. Jin H, Han H, Song G, Oh HJ and Lee BY: Anti-obesity effects of GABA in C57BL/6J mice with high-fat diet-induced obesity and 3T3-L1 adipocytes. Int J Mol Sci 25: 995, 2024.
2. Kang SA and Yu HS: Anti-obesity effects by parasitic nematode (*Trichinella spiralis*) total lysates. Front Cell Infect Microbiol 13: 1285584, 2024.
3. Shi Q, Wang Y, Hao Q, Vandvik PO, Guyatt G, Li J, Chen Z, Xu S, Shen Y, Ge L, *et al*: Pharmacotherapy for adults with overweight and obesity: A systematic review and network meta-analysis of randomised controlled trials. Lancet 399: 259-269, 2022.
4. Huttunen R and Syrjänen J: Obesity and the outcome of infection. Lancet Infect Dis 10: 442-443, 2010.
5. Muscogiuri G, Pugliese G, Laudisio D, Castellucci B, Barrea L, Savastano S and Colao A: The impact of obesity on immune response to infection: Plausible mechanisms and outcomes. Obes Rev 22: e13216, 2021.
6. Nour TY and Altintaş KH: Effect of the COVID-19 pandemic on obesity and its risk factors: A systematic review. BMC Public Health 23: 1018, 2023.
7. Tak YJ and Lee SY: Anti-obesity drugs: Long-term efficacy and safety: An updated review. World J Mens Health 39: 208-221, 2021.
8. Sun NN, Wu TY and Chau CF: Natural dietary and herbal products in anti-obesity treatment. Molecules 21: 1351, 2016.
9. Yan WJ, Yang TG, Liao R, Wu ZH, Qin R and Liu H: Complete chloroplast genome sequence of *Chrysosplenium macrophyllum* and *Chrysosplenium flagelliferum* (*Saxifragaceae*). Mitochondrial DNA B Resour 5: 2040-2041, 2020.
10. Choi HA, Ahn SO, Lim HD and Kim GJ: Growth suppression of a gingivitis and skin pathogen *Cutibacterium* (*Propionibacterium*) acnes by medicinal plant extracts. Antibiotics (Basel) 10: 1092, 2021.
11. Jakab J, Miškić B, Mikšić S, Juranić B, Ćosić V, Schwarz D and Včev A: Adipogenesis as a potential anti-obesity target: A review of pharmacological treatment and natural products. Diabetes Metab Syndr Obes 14: 67-83, 2021.
12. Madsen MS, Siersbaek R, Boergesen M, Nielsen R and Mandrup S: Peroxisome proliferator-activated receptor γ and C/EBPα synergistically activate key metabolic adipocyte genes by assisted loading. Mol Cell Biol 34: 939-954, 2014.
13. Barak Y, Nelson M, Ong E, Jones Y, Ruiz-Lozano P, Chien K, Koder A and Evans R: PPAR gamma is required for placental, cardiac, and adipose tissue development. Mol Cell 4: 585-595, 1999.
14. Rosen E, Sarraf P, Troy A, Bradwin G, Moore K, Milstone D, Spiegelman B and Mortensen R: PPAR gamma is required for the differentiation of adipose tissue in vivo and in vitro. Mol Cell 4: 611-617, 1999.
15. Duan SZ, Ivashchenko CY, Whitesall SE, D'Alecy LG, Duquaine DC, Brosius FC III, Gonzalez F, Vinson C, Pierre MA, Milstone DS and Mortensen RM: Hypotension, lipodystrophy, and insulin resistance in generalized PPARgamma-deficient mice rescued from embryonic lethality. J Clin Invest 117: 812-822, 2007.
16. Imai T, Takakuwa R, Marchand S, Dentz E, Bornert JM, Messaddeq N, Wendling O, Mark M, Desvergne B, Wahli W, *et al*: Peroxisome proliferator-activated receptor gamma is required in mature white and brown adipocytes for their survival in the mouse. Proc Natl Acad Sci USA 101: 4543-4547, 2004.
17. Linhart HG, Ishimura-Oka K, DeMayo F, Kibe T, Repka D, Poindexter B, Bick RJ and Darlington GJ: C/EBPalpha is required for differentiation of white, but not brown, adipose tissue. Proc Natl Acad Sci USA 98: 12532-12537, 2001.
18. Wang N, Finegold M, Bradley A, Ou C, Abdelsayed S, Wilde M, Taylor L, Wilson D and Darlington G: Impaired energy homeostasis in C/EBP alpha knockout mice. Science 269: 1108-1112, 1995.
19. Yang J, Croniger C, Lekstrom-Himes J, Zhang P, Fenyus M, Tenen D, Darlington G and Hanson R: Metabolic response of mice to a postnatal ablation of CCAAT/enhancer-binding protein alpha. J Biol Chem 280: 38689-38699, 2005.
20. Rosen E, Hsu CH, Wang X, Sakai S, Freeman M, Gonzalez F and Spiegelman B: C/EBPalpha induces adipogenesis through PPARgamma: A unified pathway. Genes Dev 16: 22-26, 2002.
21. Rosen ED and MacDougald OA: Adipocyte differentiation from the inside out. Nat Rev Mol Cell Biol 7: 885-896, 2006.
22. Chang E and Kim CY: Natural products and obesity: A focus on the regulation of mitotic clonal expansion during adipogenesis. Molecules 24: 1157, 2019.
23. Yang XD, Ge XC, Jiang SY and Yang YY: Potential lipolytic regulators derived from natural products as effective approaches to treat obesity. Front Endocrinol (Lausanne) 13: 1000739, 2022.
24. Saponaro C, Gaggini M, Carli F and Gastaldelli A: The subtle balance between lipolysis and lipogenesis: A critical point in metabolic homeostasis. Nutrients 7: 9453-9474, 2015.
25. Song Z, Xiaoli AM and Yang F: Regulation and metabolic significance of de novo lipogenesis in adipose tissues. Nutrients 10: 1383, 2018.
26. Brejchova K, Radner FPW, Balas L, Paluchova V, Cajka T, Chodounska H, Kudova E, Schratter M, Schreiber R, Durand T, *et al*: Distinct roles of adipose triglyceride lipase and hormone-sensitive lipase in the catabolism of triacylglycerol estolides. Proc Natl Acad Sci USA 118: e2020999118, 2021.

27. Mottillo EP and Granneman JG: Intracellular fatty acids suppress β-adrenergic induction of PKA-targeted gene expression in white adipocytes. Am J Physiol Endocrinol Metab 301: E122-E131, 2011.
28. Chakrabarti P, English T, Karki S, Qiang L, Tao R, Kim J, Luo Z, Farmer SR and Kandror KV: SIRT1 controls lipolysis in adipocytes via FOXO1-mediated expression of ATGL. J Lipid Res 52: 1693-1701, 2011.
29. Barbato DL, Aquilano K, Baldelli S, Cannata SM, Bernardini S, Rotilio G and Ciriolo MR: Proline oxidase-adipose triglyceride lipase pathway restrains adipose cell death and tissue inflammation. Cell Death Differ 21: 113-123, 2014.
30. Granneman JG, Moore HP, Krishnamoorthy R and Rathod M: Perilipin controls lipolysis by regulating the interactions of AB-hydrolase containing 5 (Abhd5) and adipose triglyceride lipase (Atgl). J Biol Chem 284: 34538-34544, 2009.
31. Contreras GA, Strieder-Barboza C and Raphael W: Adipose tissue lipolysis and remodeling during the transition period of dairy cows. J Anim Sci Biotechnol 8: 41, 2017.
32. Straub BK, Stoeffel P, Heid H, Zimbelmann R and Schirmacher P: Differential pattern of lipid droplet-associated proteins and de novo perilipin expression in hepatocyte teratogenesis. Hepatology 47: 1936-1946, 2008.
33. Temprano A, Sembongi H, Han GS, Sebastián D, Capellades J, Moreno C, Guardiola J, Wabitsch M, Richart C, Yanes O, *et al*: Redundant roles of the phosphatidate phosphatase family in triacylglycerol synthesis in human adipocytes. Diabetologia 59: 1985-1994, 2016.
34. Shin H, Shi H, Xue B and Yu L: What activates thermogenesis when lipid droplet lipolysis is absent in brown adipocytes?. Adipocyte 7: 143-147, 2018.
35. Nguyen VTT, Vu VV and Pham PV: Brown adipocyte and browning thermogenesis: Metabolic crosstalk beyond mitochondrial limits and physiological impacts. Adipocytes 12: 2237164, 2023.
36. Van der Vaart JI, Boon MR and Houtkooper RH: The role of AMPK signaling in brown adipose tissue activation. Cells 10: 1122, 2021.
37. Gulyaeva O, Dempersmier J and Sul HS: Genetic and epigenetic control of adipose development. Biochim Biophys Acta Mol Cell Biol Lipids 1864: 3-12, 2019.
38. Hirayama D, Iida T and Nakase H: The phagocytic function of macrophage-enforcing innate immunity and tissue homeostasis. Int J Mol Sci 19: 92, 2018.
39. Navegantes KC, de Souza Gomes R, Pereira PAT, Czaikoski PG, Azevedo CHM and Monteiro MC: Immune modulation of some autoimmune diseases: The critical role of macrophages and neutrophils in the innate and adaptive immunity. J Transl Med 15: 36, 2017.
40. Lagos LS, Luu TV, De Haan B, Faas M and De Vos P: TLR2 and TLR4 activity in monocytes and macrophages after exposure to amoxicillin, ciprofloxacin, doxycycline and erythromycin. J Antimicrob Chemother 77: 2972-2983, 2022.
41. Wu J, Mo J, Xiang W, Shi X, Guo L, Li Y, Bao Y and Zheng L: Immunoregulatory effects of Tetrastigma hemsleyanum polysaccharide via TLR4-mediated NF-κB and MAPK signaling pathways in Raw264.7 macrophages. Biomed Pharmacother 161: 114471, 2023.